

EFFECTS OF INTERACTION BETWEEN STRESS AND TEMPERATURE ON ULTRASOUND VELOCITY

Wallace L. Anderson
Electrical Engineering Department
University of Houston
Houston, TX 77004

INTRODUCTION

The work described here is part of a program to explore the possibility of employing a new concept for ultrasonic nondestructive evaluation of subsurface residual stress in metals. Theory indicates its potential applicability to characterization of stress to depths of 1-2 cm or more. The method employs a measurement of time variations in velocity in response to the inducement of time-varying thermal gradients within the stress region. The physical principle, as discussed below, is an interaction between stress, temperature and velocity.

Experimental results have been obtained recently for applied compressive stress in aluminum, with heat applied using an oxyacetylene torch. Ultrasonic velocity variation with time in a bar about 5 cm long is detected by demodulation of VCO frequency in a pulse phase-lock loop system. A PC-based data acquisition system is employed for frequency demodulation and data storage.

THEORY

The theory of the concept has been presented previously [1,2], but a brief outline will be given here for convenience. The physical basis is a phenomenon which can be expressed as

$$\frac{dv}{du} = -k_1 + k_2\sigma \quad (1)$$

where v is velocity, u is temperature, σ is stress and k_1 and k_2 are positive constants. This relationship was explored extensively by K. Salama over a range of temperatures with uniform applied and residual stress in specimens of aluminum, steel and copper [3,4,5]. The relationship holds for both compressional and transverse waves, although with different constants.

Theoretical study by Anderson [1] showed that for a one-dimensional system, if stress is considered to be a function of position (i.e., $\sigma = \sigma(x)$), it should be possible to infer $\sigma(x)$ from time variations in velocity following the application of controlled transient thermal excitation to the metal. The reasoning goes as follows. The spatially averaged

acoustic velocity over a length L for a one-dimensional geometry is given by

$$\langle v(t) \rangle = \frac{1}{L} \int_0^L v(x,t) dx, \quad (2)$$

where $v(x,t)$ is the internal velocity, assumed to depend on both distance and time through a dependence on temperature and stress. Then if $u(x,t)$ is the relative temperature in the material, we can separate the effect of stress by taking the time derivative:

$$\frac{d\langle v(t) \rangle}{dt} = \frac{1}{L} \int_0^L \frac{\partial v}{\partial u} \frac{\partial u}{\partial t} dx. \quad (3)$$

Substituting the partial derivative equivalent of Eq.(1) into (3) gives

$$\frac{d\langle v(t) \rangle}{dt} = \frac{1}{L} \int_0^L [-k_1 + k_2 \sigma(x)] \frac{\partial u}{\partial t} dx. \quad (4)$$

We shall assume that the "heat input" is specified by $\partial u / \partial x = -\delta(t)$ on the boundary $x = 0$, and that $\partial u / \partial x = 0$ at $x = L$. (See Fig.1) Then the homogeneous diffusion equation applies for $t > 0$, and we can set $\partial u / \partial t = c \partial^2 u / \partial x^2$ under that condition, where c is the diffusivity constant. We obtain

$$\frac{d\langle v(t) \rangle}{dt} = -\frac{ck_1}{L} \delta(t) + \frac{k_2}{cL} \int_0^L \sigma(x) \frac{\partial^2 u}{\partial x^2} dx. \quad (5)$$

Under the boundary conditions specified above, the temperature is given by

$$u(x,t) = \frac{1}{\sqrt{\pi ct}} [e^{-x^2/4ct} + \sum_{n=1}^{\infty} e^{-(2nL+x)^2/4ct} + e^{-(2nL-x)^2/4ct}]. \quad (6)$$

The first term is a good approximation for our purposes. Equation (5) can be easily solved for the rectangular stress profile $\sigma(x) = \Delta$ (a constant) between x_1 and x_2 , and zero otherwise. The result is

$$\frac{d\langle v(t) \rangle}{dt} = -\frac{ck_1}{L} \delta(t) + \frac{k_2 \Delta}{L \sqrt{4\pi ct^3}} (x_1 e^{-x_1^2/4ct} - x_2 e^{-x_2^2/4ct}). \quad (7)$$

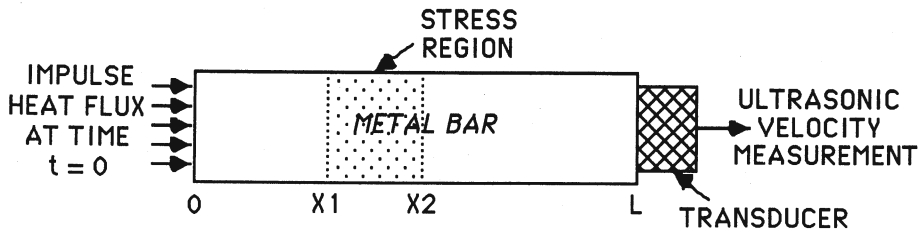


Fig. 1. One-dimensional setup for study of ultrasonic velocity deviations due to stress and impulse heat input.

Instrumentation used in current experiments gives $\langle v(t) \rangle$ itself, so we integrate Eq. (7), obtaining

$$\langle v(t) \rangle = v_0 - \frac{ck_1}{L} U(t) + \frac{k_2 \Delta}{L \sqrt{4\pi c}} \int_0^t \frac{1}{t^{3/2}} \left(x_1 e^{-x_1^2/4ct} - x_2 e^{-x_2^2/4ct} \right) dt, \quad (8)$$

where $U(t)$ is the unit step function, and v_0 is the velocity at ambient temperature. It can be noted that if the stress is zero throughout the region, the third term will be zero, and the velocity after $t = 0$ will be constant at $(v_0 - ck_1/L)$. The general appearance of Eq. (8) for non-zero stress is shown in Fig. 2 for $c = 0.95$ (aluminum) and $k_2 \Delta / k_1 = 0.6$. Two different choices of (x_1, x_2) are shown to illustrate the effect of changing the location of the stress region.

When the heat flux is not well-represented by a δ -function, we can characterize the experimental result as the convolution of $\langle v(t) \rangle$ with a "pulse" function $p(t)$, representing the actual heat flux, i.e.,

$$w(t) = \langle v(t) \rangle * p(t) = \int \langle v(t) \rangle p(t-\lambda) d\lambda, \quad (9)$$

with the integral taken over all λ . The result of the convolution is of course a "smoother" version of $\langle v(t) \rangle$. The initial drop in velocity due to the sudden influx of heat is no longer instantaneous, but lasts as long as the duration of $p(t)$. Subsequent variation of $\langle v(t) \rangle$ with time due to interaction of heat with the stress is similarly broadened.

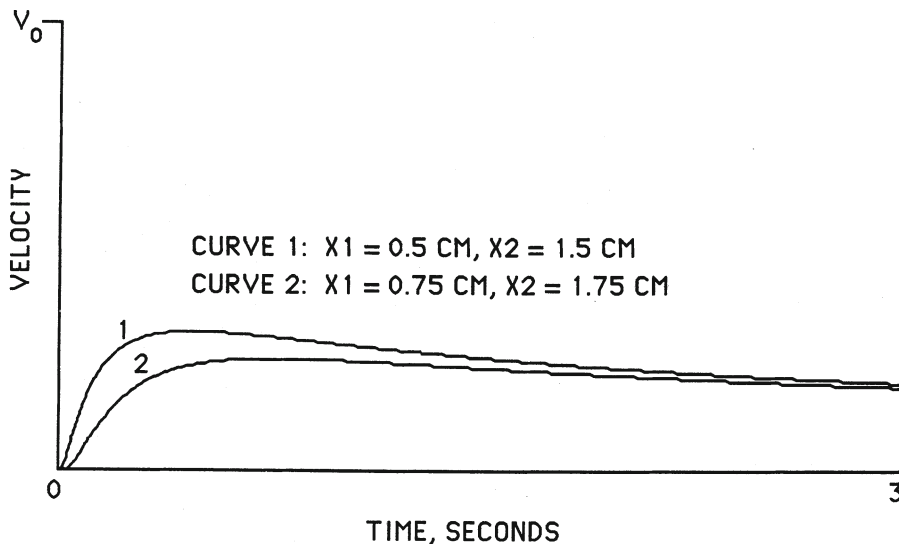


Fig. 2. Theoretical curves representing Eq. (8) for two rectangular stress profiles, one slightly (0.25 cm) displaced from the other.

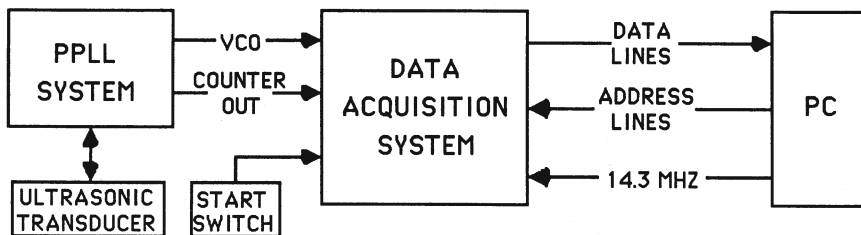


Fig. 3. Experimental system for measurement and storage of time-varying ultrasonic velocity data.

EXPERIMENTS

Electronics

Measurement of the time-varying velocity is accomplished using the system of Fig. 3. A MicroUltrasonics pulsed phase lock loop (PPLL) [6] generates and receives ultrasonic pulses of preselected length, generally amounting to around 5-15 cycles of the operating frequency (in the range 2-5 MHz). The pulses are gated on at a rate of a few hundred per second. The frequency of the oscillator (VCO) is controlled in the usual way by a feedback voltage representing phase error between pulse echoes and the continuously running VCO. Due to certain characteristics of the PPLL circuitry, this feedback voltage does not follow frequency deviation very precisely, so a PC-based data acquisition system has been designed to perform the dual functions of frequency demodulation and data storage.

Figure 4 is a block diagram of this system [7]. An adjustable local oscillator produces a voltage which is mixed with that of the VCO to produce a nominal difference frequency, usually around 10 kHz. The resultant waveform is shaped for TTL compatibility, divided by two and used to gate the 14.3 MHz clock voltage of the PC into a high speed counter. Counter output in the form of a 16-bit word for each gating interval (this interval being equal to the period of the difference frequency) is

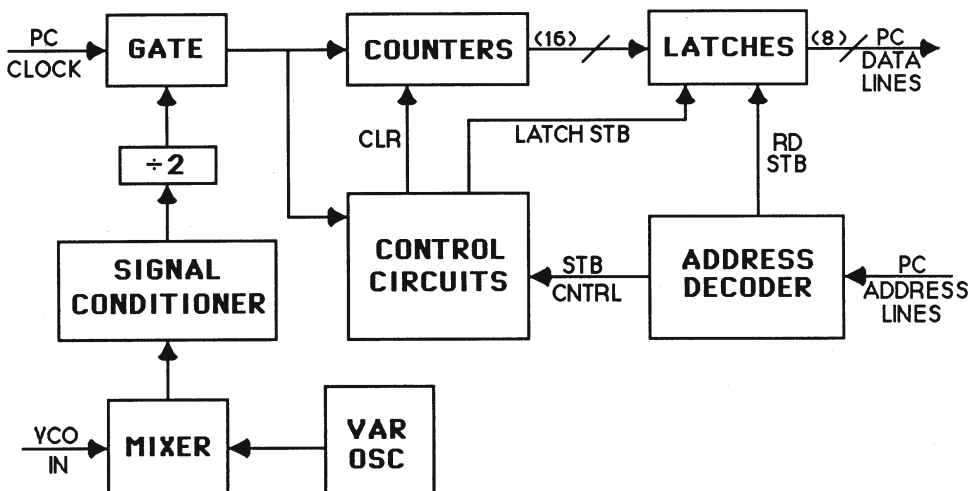


Fig. 4. The data acquisition system.

transmitted to the PC and stored on floppy disk. Thus the VCO frequency is effectively sampled at a rate of around 5000/sec. The frequency resolution is then f_d^2/f_c , where f_d is the difference frequency and f_c the clock frequency (14.3 MHz in this case). Phase jitter in the low-frequency waveform results in substantial random noise, amounting to about 20-30 Hz; however the sampling rate allows a sufficient extent of adjacent sample averaging to give a high degree of smoothing while still allowing more than enough time resolution. For example, 50-sample averaging at the 5000/sec rate gives a resolution of .01 seconds.

Signal Processing

Owing to the fact of its being obtained as a result of a heat diffusion process, one should not expect that the signal would have a high information content in most circumstances of interest. The signal processing method must therefore operate on the measured data as efficiently as possible. Two approaches to this problem are being studied: one is based on a generalized matrix inversion with constraints; the other is a parameter fitting technique.

For the matrix inversion, the signal (which could be either $\langle v(t) \rangle$ or some processed version thereof) is discretized with respect to time, resulting in a signal vector \mathbf{S} with elements $s(t_i)$, $i = 1, 2, 3, \dots, N$. The stress profile, $\sigma(x)$, is also put into discrete form with respect to values of x , giving a vector Σ with elements $\sigma(x_j)$, $j = 1, 2, 3, \dots, M$. Similarly $\partial u / \partial t$ is discretized with respect to both x and t to give an $N \times M$ ($N \geq M$) matrix \mathbf{G} with elements G_{ij} . For the simplest assumption concerning the statistics of the noise, the estimate of Σ then proceeds according to the formula [8]

$$\hat{\Sigma} = [\mathbf{G}^T \mathbf{G}]^{-1} \mathbf{G}^T \mathbf{S}. \quad (10)$$

Because of the limited information content of the signal vector in this case, this inversion tends to be quite unstable unless N is relatively small [9]. Much improvement can be gained, however, if knowledge of the nature of \mathbf{S} can be incorporated in the form of one or more constraints. One such constraint applicable for compressive stress is "positivity" i.e., $\sigma(x) \geq 0$ (or "negativity" for tensile stress), and trial calculations using simulated data with added Gaussian noise show that this is an extremely effective way to stabilize the inversion. However, the computational procedure is nonlinear and iterative, and considerably more complex than that for the unconstrained solutions [10].

A second approach is based on representing the stress profiles in terms of standard "shapes". For the simplest shapes (e.g., Gaussian, Lorentzian, parabolic, rectangular) three parameters (say, A , w and c) are sufficient to characterize magnitude, width and center location. One then seeks to minimize the integral of the squared difference between the theoretical and measured signals:

$$F(A, w, c) = \int_0^T [s(t, A, w, c) - s_m(t)]^2 dt, \quad (12)$$

(or its equivalent in discrete form) with respect to variations in A , w , and c . Preliminary results with simulated data and noise show that this approach may be quite effective, but as yet a detailed comparison between this and the matrix inversion approach has not been made.

Heat Input

It is evident that the greatest possible thermal gradients in the metal and therefore the maximum signal responses to stress will occur for a δ -function heat input. This can be achieved to a good degree of approximation in this case for a heat source consisting of a pulsed laser with pulse duration less than a millisecond or so; however, such a source is not available to us at the present time. It has therefore been necessary to employ a torch, with flame applied to the metal bar end for a brief interval. Both a "MAPP" torch and an oxyacetylene torch have been used. The results shown in the next section were obtained using the oxyacetylene torch, which is apparently about four or five times hotter than the other. At present the configuration of the specimen and means of stress application make it awkward to use mechanical shuttering for timing of heat exposure, so for the time being the torch is hand-held and passed by the end of the specimen in a smooth motion. Despite the uncertainties that might be expected for this procedure, the records show a fair amount of uniformity, with time duration for the initial velocity change (and, therefore, the exposure time itself) generally close to 1/4 second.

RESULTS

Stress was applied over a region from 1 cm to 2.25 cm from the heat input end of an aluminum bar, using the configuration of Fig. 5. Stress values were 0, 3.2, 4.8, 5.6 and 8.0 kpi, as indicated for the representative results shown in Fig. 6. A fairly reasonable degree of proportionality to stress is seen, despite a certain amount of noise in the measurements. In addition, heat application often spilled over to the sides and stress contact bars, resulting in an "input" heat flux after the initial drop of velocity. In the case of zero stress, firm contact was maintained between the specimen and the contact bars, so that heat loss through the latter would not be appreciably different than for the other stress values. Since heat input amount varied as much as 20% or so from one measurement to the next, the curves have been all been normalized with respect to initial velocity decrease. Also, the reference point for alignment in time was chosen to be the point of maximum slope during this interval of velocity change. The widths of the velocity de-

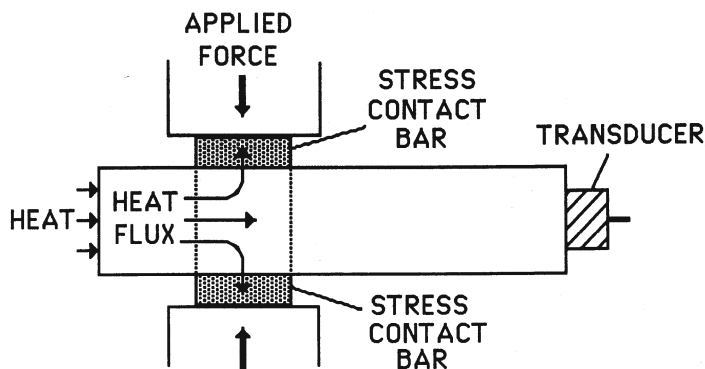


Fig. 5. Application of stress. Because of appreciable heat flux out of the bar, one-dimensional theory is not strictly applicable.

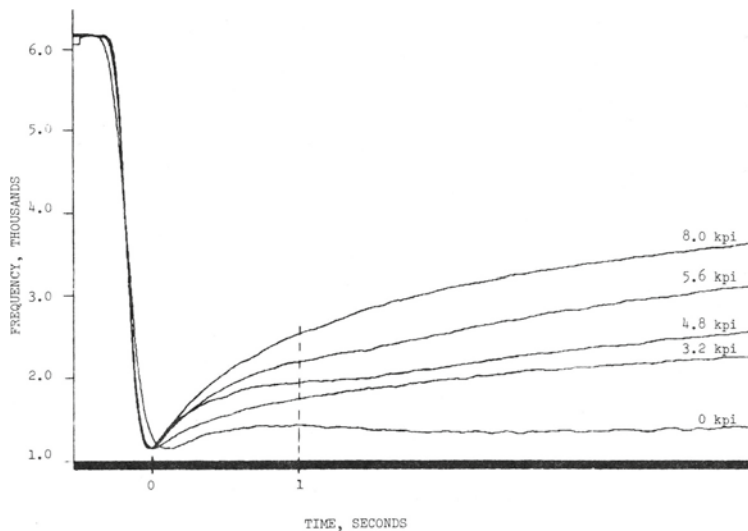


Fig. 6. Experimental results. Sampling rate was about 5000/sec, and 100-point adjacent-sample averaging was used.

crease regions are fairly uniform at around 1/4 second, as noted previously. The amount of change in this region indicates an energy input in the neighborhood of 50 Joule/cm² during heat exposure. Because the horizontal scale is linear with respect to sampling points and since the sampling rate varies with the difference frequency, it is nonlinear with time. As a result, the time scale of the different curves is not quite the same, and so the superposition of the curves is not strictly justified. The approximate location of the 1-second point (after minimum) has been sketched in for reference.

The theoretical model for these experimental results is obviously Eq. (9), although of course the precise shape of $p(t)$ is unknown at present. A discrepancy with theory exists, however, in that the magnitude of velocity deviation (e.g., 500 cm/sec at 1 sec for 8 kpi) following the initial drop is significantly greater for experiment than predicted theoretically. At present, it is believed that this is due to the thermal gradient in the stress region being larger than predicted by the one-dimensional theory, as a result of conduction of heat through the stress contact regions. Tests are underway using less thermally conducting contacts to see if the discrepancy is due to this factor.

CONCLUSIONS

Preliminary experimental results now clearly indicate the viability of a new concept for nondestructive characterization of subsurface residual stress in metals. The method requires measurement of temporal variations in ultrasonic velocity following transient application of heat to the surface of the metal.

ACNOWLEDGEMENT

This work was supported by the Army Research Office.

REFERENCES

1. W. L. Anderson, "Ultrasonic Velocity Dependence on Stress and Pulsed Heat Energy", *Review of Progress in Quantitative Nondestructive Evaluation*, eds. D. O. Thompson and D. E. Chimenti, Plenum Press, N. Y. (1984), Vol. 3B, pp. 1157-1164.
2. W. L. Anderson, Y. Motiwala and M. S. Toth, "Detection of Subsurface Stress in Metals Using Ultrasound and Time-varying Thermal Gradients", *Proceedings IEEE 1986 Ultrasonics Symposium*, Vol. 1, pp. 531-533, 1986.
3. K. Salama and C. K. Ling, *J. Appl Phys.* 51, 1505 (1980).
4. K. Salama, C. K. Ling and J. J. Wang, *Experimental Techniques* 5, 14 (1981).
5. K. Salama, G. C. Barber and N. Chandrasekaran, *Proc. IEEE Ultrasonics Symposium*, p. 877 (1982).
6. J. Heyman, "Ultrasonic Measurement of Axial Stress," *ASTM J. of Testing and Eval.* 10, no.5, pp. 202-211, Sept. 1982.
7. W. L. Anderson, Y. Motiwala and C. E. Jensen, "Thermal Effects on Ultrasonic Waves in the Presence of Stress", *Proceedings Ultrasonics International 87*, Butterworth & Co. Ltd., 1987, pp. 532-536.
8. T. O. Lewis and P. L. Odell, *Estimation in Linear Models*, Prentice-Hall (1971), p. 52.
9. S. Twomey, "On the Numerical Solution of Fredholm Integral Equations of the First Kind by the Inversion of the Linear System Produced by Quadrature," *J. Assoc. Comput. Mach.* 10, 97 (1963).
10. A. Ben-David, B. M. Herman and J. A. Reagan, "Inverse Problem and the Pseudoempirical Orthogonal Function Method of Solution. 1. Theory," *Appl. Opt.* 27, 1235 (1988).